Document downloaded from:

http://hdl.handle.net/10251/37892

This paper must be cited as:

Reig Cerdá, L.; Amigó Borrás, V.; Busquets Mataix, DJ.; Calero, JA. (2011). Stiffness variation of porous titanium developed using space holder method. Powder Metallurgy. 54(3):389-392. doi:10.1179/003258910X12707304455068.

The final publication is available at

http://dx.doi.org/10.1179/003258910X12707304455068

Copyright Maney Publishing

Manuscript (NOT PDF FILE AT REVISE STAGE)
Click here to download Manuscript (NOT PDF FILE AT REVISE STAGE): Manuscript_Porous titanium stiffness variation_POM162

STIFFNESS VARIATION OF POROUS TITANIUM DEVELOPED USING THE SPACE HOLDER METHOD

L. REIG[a], V. AMIGÓ[b], D. BUSQUETS[b] , J.A. CALERO[c]

[a] Departamento de Ingeniería Mecánica y Construcción, Universidad Jaime I de Castellón. Av. de Vicent Sos Baynat, s/n, 12071 Castelló de la Plana, Spain.
lreig@emc.uji.es

[b] Departamento de Ingeniería Mecánica y de Materiales, Universidad Politécnica de Valencia, Camino de Vera s/n, 46022, Valencia, Spain.
vamigo@mcm.upv.es; dbusquets@mcm.upv.es

[c] Aleaciones de Metales Sinterizados S.A. (AMES), San Vicenç dels Horts, Barcelona, Spain.
jacalero@alme.ames.es

Corresponding author: lreig@emc.uji.es, Phone: +34 963877623

ABSTRACT

The excellent properties of titanium have resulted in its generalised use for bone implants. However, titanium is very stiff in comparison with human cortical bone and this creates problems of bone weakening and loosening of the implant. This article discusses the mechanical properties (flexural and compressive strength, and stiffness) of porous Ti-6Al-4V specimens developed using the space holder method. These properties are examined relative to the production process parameters: compacting pressure and sintering time; as well as temperature, and the addition of spacer and its particle size. It is seen that when spacer is added, compressive strength decreases with the application of compacting pressure – and that these are the most influential parameters. The developed pieces show a closed and unconnected porosity. Small additions of spacer (25% volume) reduce stiffness to around half of that shown by the solid material; and the resulting pieces are strong enough to be used as bone substitute.

Keywords: porous Ti-6Al-4V, space holder, bending strength, compression strength, stiffness.

1. Introduction

The excellent properties of titanium make it an ideal candidate for use as a bone graft. However, production is difficult because vacuum techniques are required to minimize reactivity with gases in the furnace. Moreover, although its stiffness (100-110 GPa)[1,11] is small when compared to other implant materials, it is still higher than human cortical bone (10-40 GPa)[1,2], and this leads to bone weakening and loosening of the implant[3] due to the stress-shielding phenomenon.
Among the various methods for reducing the stiffness of the implant[4-7] the development of porous pieces with the spacer method is one of the most widely used[8, 9]. Porosity is generated by removing spacer that was mixed together and compacted with the base material. The aim of this work is to develop specimens of porous Ti-6Al-4V using the spacer method and measure the change in resistance to bending, compression, and stiffness – as influenced by the process parameters (compacting pressure, sintering time and temperature, addition of spacer and particle size).

2. Experimental procedure

2.1 Development of porous specimens using the spacer method

Specimens were developed following procedures described in previous works[10]. Titanium alloy selected for this research was Ti-6Al-4V powder produced by hydration-dehydration (HDH). The powder was supplied by Se-Jong Materials, who also provided its chemical composition[10] and sieve analysis (<45 μm). Ammonium bicarbonate was used a spacer, and the bicarbonate was ground and sieved to three different sizes (125-250 μm , 250-500 μm, and 500-1000 μm). Given the irregular morphology of both materials[10], the strength acquired after compacting was sufficient to enable manipulation to remove the spacer.

After mixing the Ti-6Al-4V and ammonium bicarbonate (% volume Ti-6Al-4V/Esp: 100-0; 75-25; 60/40; 45/55; 30/70), the mixture was compacted to 100, 200 and 300 MPa in a 100-ton uniaxial hydraulic press at a rate of 3000 N/s after contact with the mix. For each combination of variables, three compression samples (Ø = 25 mm, h ≈ 27 mm) and five bending samples (32x12x6 mm^3) were produced.

After the spacer was removed, the samples were sintered in a vacuum at temperatures of 1300 ± 25 ºC for periods of one, two, and four hours[10].

2.2 Analysis of the porous specimens

After metallographic preparation, the samples were examined under a Nikon SMZ800 stereo optical microscope, a MicroPhoto Nikon FX microscope, and a JEOL JSM6300 scanning electron microscope equipped with an Oxford Instruments EDX 6508 detector. The density (ρ*) and porosity of the sintered material were determined by measuring the mass and dimensions. The solid density of (ρ_S) 4.42 g/cm^3 was used to measure the relative density ($\rho_r = \rho^*/\rho_S$)[11].

Strength and flexural stiffness were measured with the three-point bend test, following ASTM E290-97a (ISO 3325:2000); and applied in an Instron 4204 machine with a crosshead speed of 0.5 mm/min. Flexural stiffness was measured using the slope of the (σ-ε) stress-strain curve (E_{FP}*), and Young's modulus formula with a maximum deflection (E_{FF}*)[8].

The compression test was performed in accordance with ASTM E9-89a, in an Instron A1340-1006 with up to 600 KN of static load and a load speed of 0.5 mm/min until achieving a relative strain of 7 mm. The compressive stiffness (E_C*) was measured by determining the slope of the stress-strain curve.

The relative stiffness ($E_r = E^*/E_S$) was calculated for each of the measuring methods by taking the rigidity of the solid (E_S) as evidenced by the samples without spacers that were compacted at the same pressure (E_{SFF}, E_{SFP}, E_{SC}). Due to the localized plasticization that occurs in porous metals in the apparently elastic region of the stress-strain curve[12], we will refer to “rigidity”, rather than the “modulus of elasticity”.

3. Results and discussion

3.1 Porosity and pore size

The produced porous specimens have a dense outer skin, with a degree of porosity that depends primarily on the volume of spacer. Unlike the TiCP porous specimens produced in a previous research, in which compaction was performed manually[8], the porosity of the Ti-6Al-4V specimens increased by between 10 and 14% after the addition of spacer[10]. This is due to the quickness of the compaction applied, which produces greater elastic recovery in the powder.

Figure 1 shows the difference between micro and macropores. While the former are the product of the powder-metallurgical process and reduced compacting pressures, the latter result from the evaporation of bicarbonate. Although spacer particles tend to coalesce, connections do not develop between all the particles – and so the porosity is not considered to be interconnected. However, the presence of connections between spacer particles means that reference cannot be made to a specific pore size. Furthermore, the mechanical properties improve as the spacer particle size reduces[10], because this size reduction enables a better distribution of the matrix powder and compacting pressure, as shown in Fig. 1.

3.2 Resistance to bending and compression

The compression results confirm observations made in previous works[10], and demonstrate the great importance of the amount of time that passes between compacting and removal of the spacer – with long delays causing weakening. Consequently, results with brittle fracture in the test specimens have been discarded.

As with resistance to bending[10], the **most influential** variables for resistance to compression are the **addition of spacer and compacting pressure.** The size of spacer particles and the thermal cycle are less influential. The effect of pressure depends on the amount of spacer added. So, bending strength generally increases in the compacting pressure when the bicarbonate content is low (<25% volume), weakening when more bicarbonate is added[10]. In contrast, compression **only increases** strength in the compacting pressure **with pieces that did not contain spacer**, see Fig. 2.

As shown in Table 1, for the same process parameters, resistance to bending is greater than resistance to compression. Although no significant differences between the relative density of the bending and compression test pieces were apparent, the size of the

compression test specimens (13.25 cm ^{3} compared to 2.3 cm ^{3} for the bending test specimens), and the high of speed of compacting, means that the pressure gradient is higher in the compression test specimen. This results in greater heterogeneity, and therefore weaker areas exist in which plastic deformation can begin. Similarly, strength generally decreases as spacer size increases, and this is caused by a less homogeneous distribution of the powder matrix and applied pressure.

Moreover, scattering in the results is also greater for bending than compression; and this scattering is more pronounced as strength increases. This is due to the greater influence of the more fragile areas, caused by the spacer particles[10], when subjected to tensile stress and/or greater force. Similarly, results are generally more scattered when particle sizes are smaller, implying an increased area of contact with the powder matrix.

Table 1. σ_y bending and compression, MPa, relative to % volume and spacer particle size. * Results eliminated where the test piece showed brittle fracture.

Ti-6Al-4V – Spacer %v	**STRESS**	**GRANULE SIZE µm**		
		125 – 250	**250 – 500**	**500 – 1000**
100 – 0	BENDING	1857 +/ - 157		
	COMPRESSION	1030 +/ - 40		
75 – 25	BENDING	No test pieces	535 +/- 110	500 +/- 40*
	COMPRESSION	No test pieces	203 +/- 20	192 +/- 10*
60 – 40	BENDING	283 +/- 33	230 +/- 50	275 +/- 5*
	COMPRESSION	109 +/- 13		91 +/- 10*
45 – 55	BENDING	103 +/- 7*		No test pieces
	COMPRESSION	92 +/- 7*		No test pieces

Since the compressive yield strength of cortical bone is between 110 and 200 MPa, with a lower value for bending[2,13,14], only specimens with 25% spacer volume can be safely used as a substitute for human cortical bone. Higher levels of spacer result in inadequate compressive strength.

The level of strength obtained is related to the relative density of the pieces according to the model (1) proposed by Gibson-Ashby[15], and based on the average strength of pieces with the same bicarbonate volume (this being the most influential variable).

$$\frac{\sigma_Y}{\sigma_S} = C\left(\frac{\rho^*}{\rho_S}\right)^n \qquad (1)$$

Where the constants C and n reflect foam parameters such as cell morphology, shape, and arrangement of the pores[16,17].

Although the model was proposed for foams (ρ_r <0.3) with an ideal microstructure[15], a good correlation has been found (R^2 = 0.99) between the relative density of porous

specimens obtained ($\rho_r = \rho^*/\rho_S$) and their relative resistance to bending ($\sigma_{YFr} = \sigma_{YF}^*/\sigma_{YFS}$) and compression ($\sigma_{YCr} = \sigma_{YC}^*/\sigma_{YCS}$). See Fig. 3.

It should be noted that in accordance with observations made during the production process, the mechanical properties of the developed porous specimens can be optimized by using the **lowest possible compacting pressure**. This facilitates a more uniform distribution and the elimination of spacer particles. Lower compacting pressure also facilitates slower compacting and this helps consolidation by reducing the elastic recovery of the material.

3.3 **Stiffness**

The stiffness of the porous pieces developed **depends primarily on the addition of spacer.** No significant differences related to the other process parameters (T, t, P, spacer size) were found.

In the same way as for strength, models were obtained correlating stiffness with the relative density of the developed specimens. Table 2 lists the coefficients obtained for the porous specimens developed in this work, as well as TiCP3 porous specimens produced in previous research[8], and results published by other authors using the spacer method to develop porous titanium.

Table 2. Correlation models based on relative stiffness and relative density.

MATERIAL	TEST	STIFFNESS MEASUREMENT	C	n	Correlation model R^2
TiCP3	Bending	Curve slope[8]	1.037	1.62	0.86
Ti-6Al-4V	Bending	Curve slope	1.172	1.60	0.97
Ti-6Al-4V	Bending	Formula	1.173	1.60	0.98
Ti-6Al-4V	Compression	Curve slope	1.136	2.19	0.96
Ideal foam		Gibson-Ashby[15]	1.000	2.00	-
TiCP	Compression	Bram et al.[9]	0.167	2.00	-
TiCP	Compression	Esen et al.[17]	1.598	4.72	0.99

In Table 2 the correlation model of relative stiffness and bending is shown independently of the measuring method used (curve slope or formula) for theTi-6Al-4V specimens developed in this work. The stiffness and compression model obtained is very similar to those proposed by Gibson and Ashby[15] and Bram[9]. This is due to similarities in the development of the pieces and measuring methods. In contrast, Esen[17] used spherical particles of titanium, so that the walls created between the macropores during sintering were smaller and demonstrated an apparently reduced cohesion. This explains why his model is more sensitive to variations in relative density. Moreover, the value close to unity obtained for the coefficient C in our models is consistent, because when the relative density is near to one, then the relative stiffness should also be near to one. Finally, it worth emphasising the small difference in coefficient C obtained for porous TiCP

specimens and Ti-6Al-4V ones. The lower value for the first samples is due to lower levels of alloying elements[18, 19].

Figure 4 shows the correlation between the models obtained for the Ti-6Al-4V specimens developed in this work and the experimental values. As with strength, the relative stiffness is higher for bending than for compression. This is related to the greater cohesion and homogeneity for the pieces obtained. So, the smaller size of the bending specimens results in a more uniform pressure distribution and less elastic recovery during compacting; and this leads to a greater cohesion and stiffness. As shown in figure 4, for pieces with a 25% volume of spacer ($\rho_r \approx 0.4$), the degree of stiffness is reduced by about 50% when compared with the solid material. This improves behaviour when placed alongside human cortical bone, and so reduces bone resorption problems.

4. Conclusions

The spacing method has enabled the development of less rigid porous Ti-6Al-4V specimens with a flexural and compressive strength that makes the material suitable for use as bone substitute. The porosity of the developed materials increases when spacer is added – and while the spacer particles are not completely connected, there is some interconnection.

The parameters that most influence the mechanical properties are the addition of spacer and compacting pressure. By contrast, there is no significant variation of properties depending on the thermal cycle, so sintering should be carried out at 1275 º C for 2 hours, which alloys sintering and enables a reduction of the consumed energy compared to the rest of thermal cycles used.

Obtained properties are slightly higher by reducing the particle size of the spacer. However, the compressive strength of human cortical bone only can be achieved with 25%v of ammonium bicarbonate at the most. These specimens are about half as stiff as the bulk material, and this improves their behaviour alongside bone and reduces problems of weakening.

The mathematical models obtained enable estimates to be made of the mechanical properties produced (resistance to bending, compression, and stiffness) as a function of relative density or the addition of spacer.

Acknowledgements

The authors wish to thank the Spanish Ministry of Science and Innovation for the support received under Project PET2008_0158_02. The translation of this article was funded by the Universidad Politécnica de Valencia.

References

[1] G. Ryan, A. Pandit, D.P. Apatsidis: *Biomaterials*, 2006, 27, 2651-2670.
[2] K. Asaoka, M. Kon: *Mater. Sci. Forum*, 2003, 426-432, 3079-3084.
[3] M. Niinomi: *J. Mech. Behav. Biomed. Mater.*, 2008, 1,1, 30-42.
[4] L. Reig, V. Amigó, D. Busquets, M.D. Salvador, J.A. Calero. Rev. de Metalurgia, 2010, in press.
[5] H.J. Rack, J.I. Qazi: *Mater. Sci. Eng. C-Biomimetic Supramol. Syst.*, 2006, 26, 8, 1269-277.
[6] G. Kotan, A.S. Bor: *Turkish J. Eng. Env. Sci.*, 2007, 31, 149-156.
[7] M. Köhl, M. Bram, H.P. Buckremer, D. Stöver: Euro PM2007, Toulouse, France, 2007, 129-134.
[8] V. Amigó, L. Reig, D. J. Busquets, J. L. Ortiz, J. A. Calero: available online since May 4th 2009, DOI: 10.1179/174329009X409697.
[9] M. Bram, S.H. Bogdanski, M. Koller, H.P. Buchkremer, D. Stover, Euro PM2005, Prague, Czech Republic, 2005, 517-522.
[10] L. Reig, V. Amigó, D. Busquets, M.D. Salvador, J.A. Calero. Sintering 2008. La Jolla, California, 2008, In press.
[11] ASM INTERNATIONAL, ASM Handbook Vol.2: Properties and Selection: Nonferrous Alloys and Special-Purpose Materials, 1170; 1990.
[12] H.P. Degischer, B. Kriszt: 'Handbook of Cellular Metals: Production, Processing, Applications', 22-184; 2002, Wiley-VCH.
[13] M. Comín, J.L. Peris, J.M. Prat, J.R. Decoz, P.M. Vera, J.V: Hoyos: 'Biomecánica de la fractura ósea y técnicas de reparación'; 66-69, 1999, Publicaciones UPV.
[14] R.B. Heimann: *CMU Journal*, 2002, 1, 23-46.
[15] L.J. Gibson, M.F. Ashby: 'Cellular Solids: Structure and Properties'; 175-231,1999, Cambridge University Press.
[16] M. Ashby, E. Michael, F. Tony, N. A. Gibson, L.J. Hutchinson, J.W. Wadley: 'Metal Foams: A Design Guide', 6-54; 2000, Butterworth - Heinemann.
[17] Z. Esen, S. Bor: *Scripta Mater.*, 2007, 56, 5, 341-344.
[18] C. Leyens, M. Peters: 'Titanium and Titanium Alloys. Fundamentals and Applications'; 1-35, 2003, Wiley-VCH.
[19] G. Lütjering, J.C. Williams: 'Titanium', 2nd edn, 13-51; 2007, Springer, Engineering Materials and Processes.

List of figures:

Fig. 1. Micrograph of porous pieces developed with different spacer particle sizes: (a) 125-250 μm; (b) 500-1000 μm.

Fig. 2. Compressive strength as a function of compaction pressure for samples with different amounts of bicarbonate.

Fig. 3. Relative resistance to bending and compression according to relative density (adjusted for developed models).

Fig. 4. Relative stiffness and compression according to relative density (adjusted for developed models).

Tables

Table 1. σ_y for bending and compression, MPa, relative to % volume and spacer particle size. *Results eliminated where the test piece showed brittle fracture.

Table 2. Correlation models based on relative stiffness and relative density.

Figure 1a: Micrograph 125-250

Click here to download high resolution image

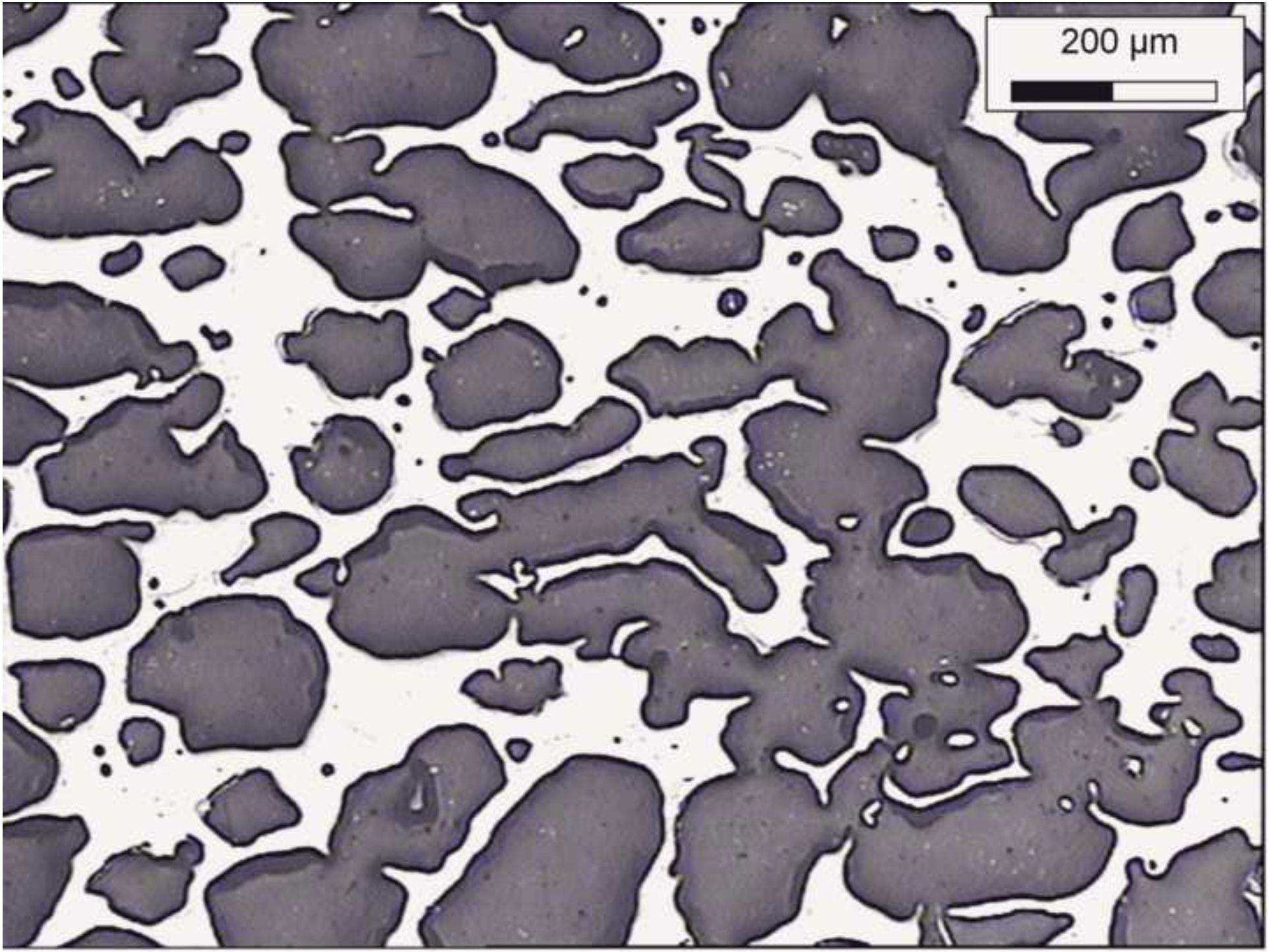

Figure 1b: Micrograph 500-1000

Click here to download high resolution image

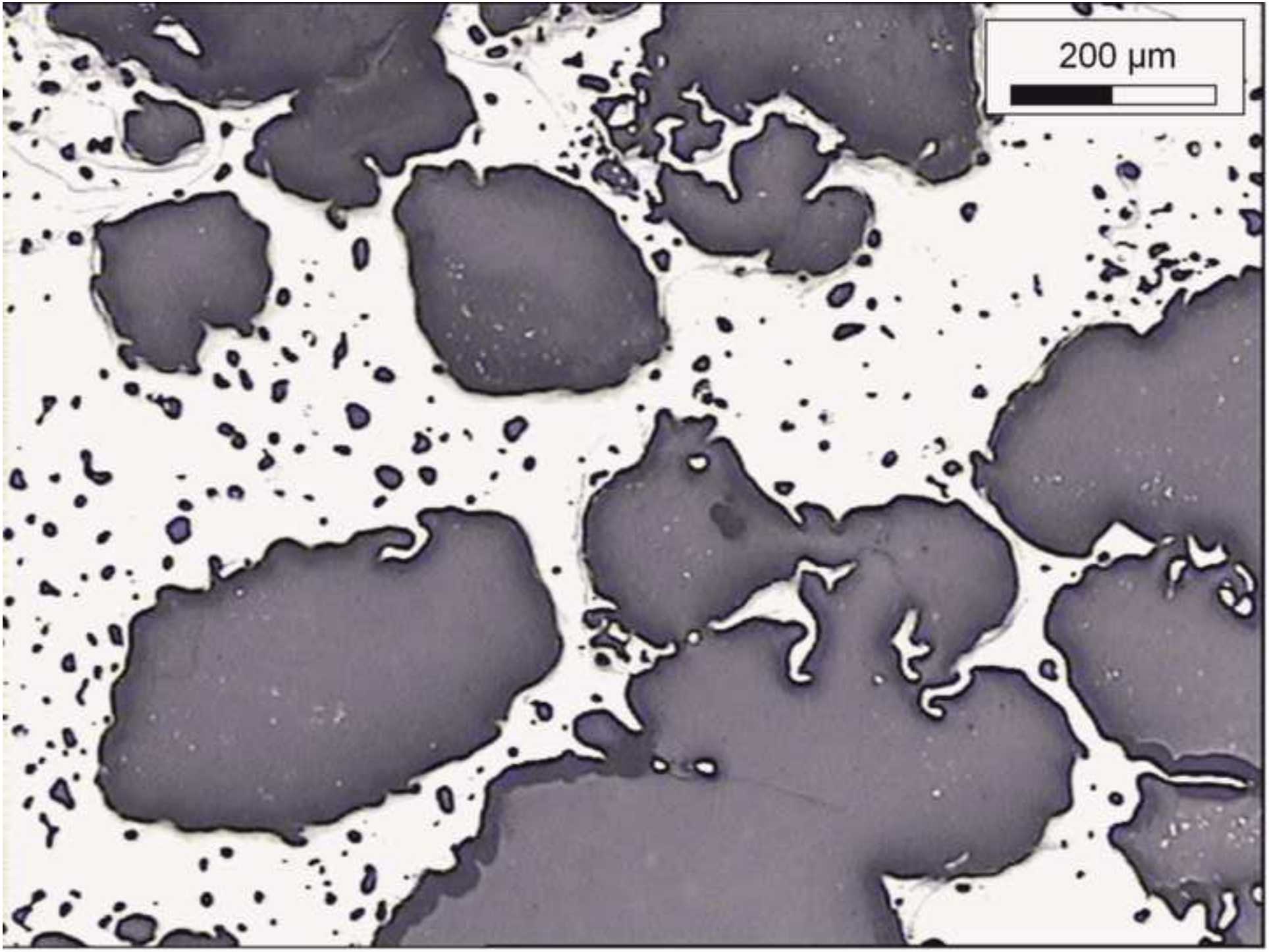

Figure 2: Compressive strength
Click here to download high resolution image

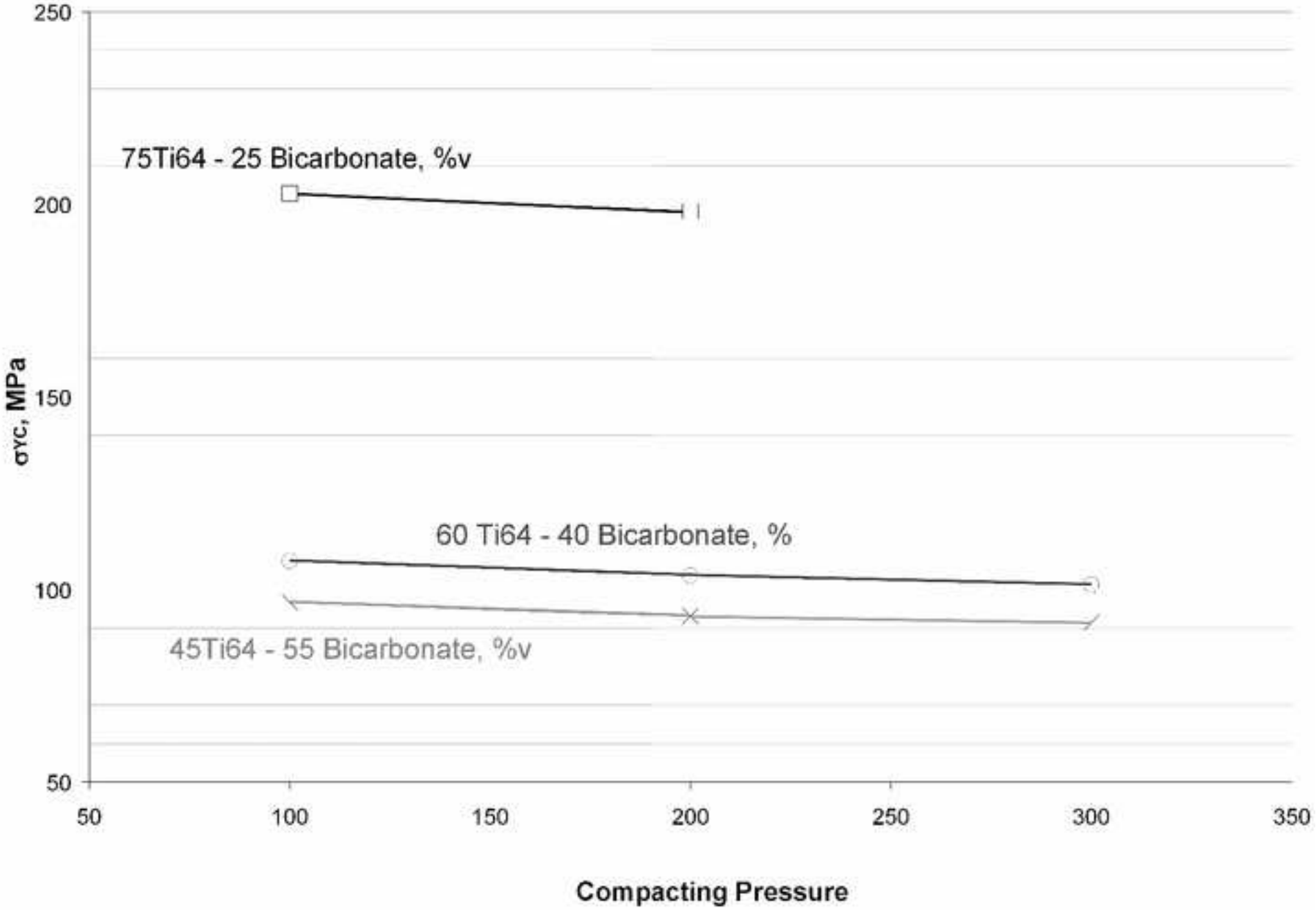

Figure 3: Relative Resistance

Click here to download high resolution image

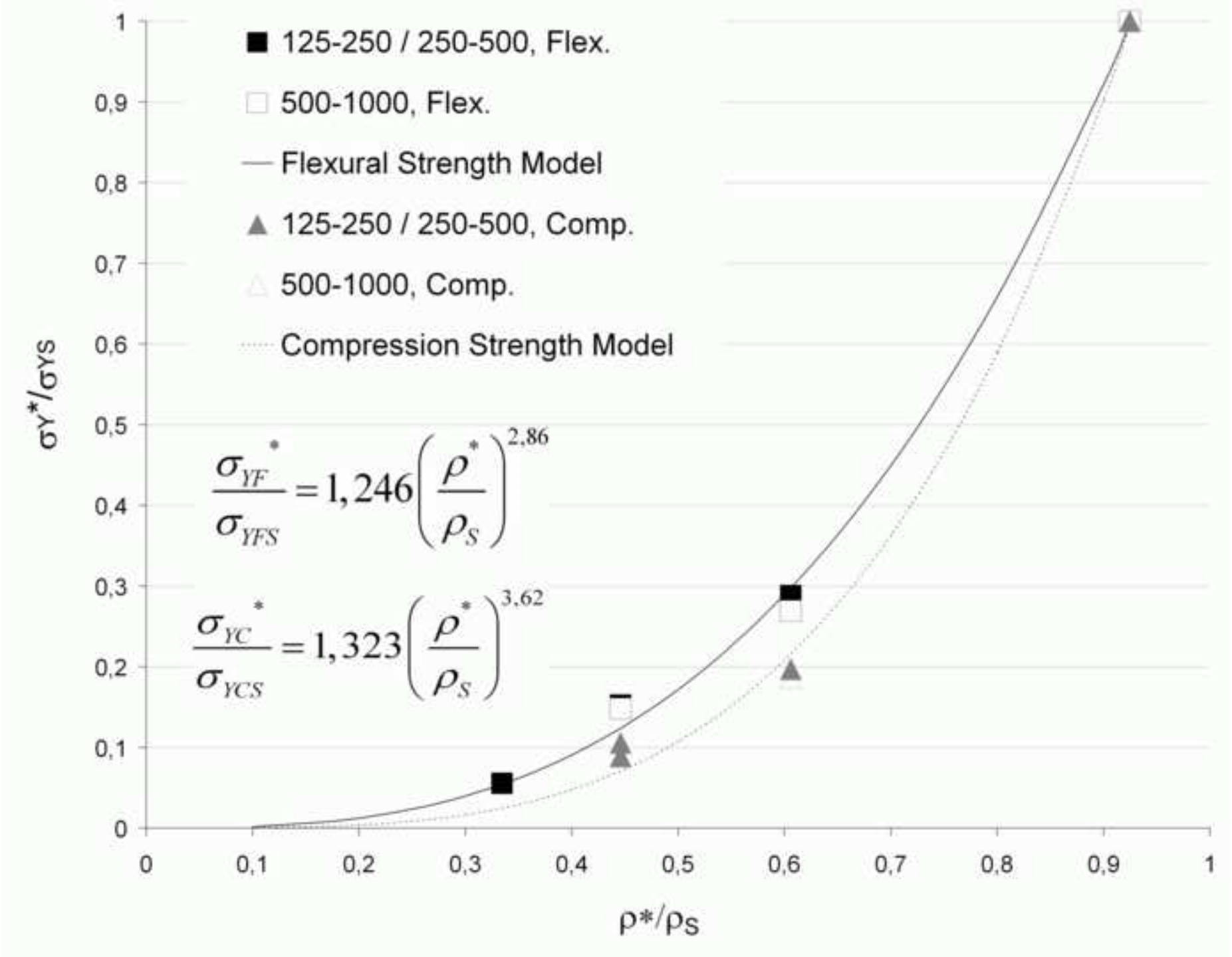

Figure 4: Relative Stiffness
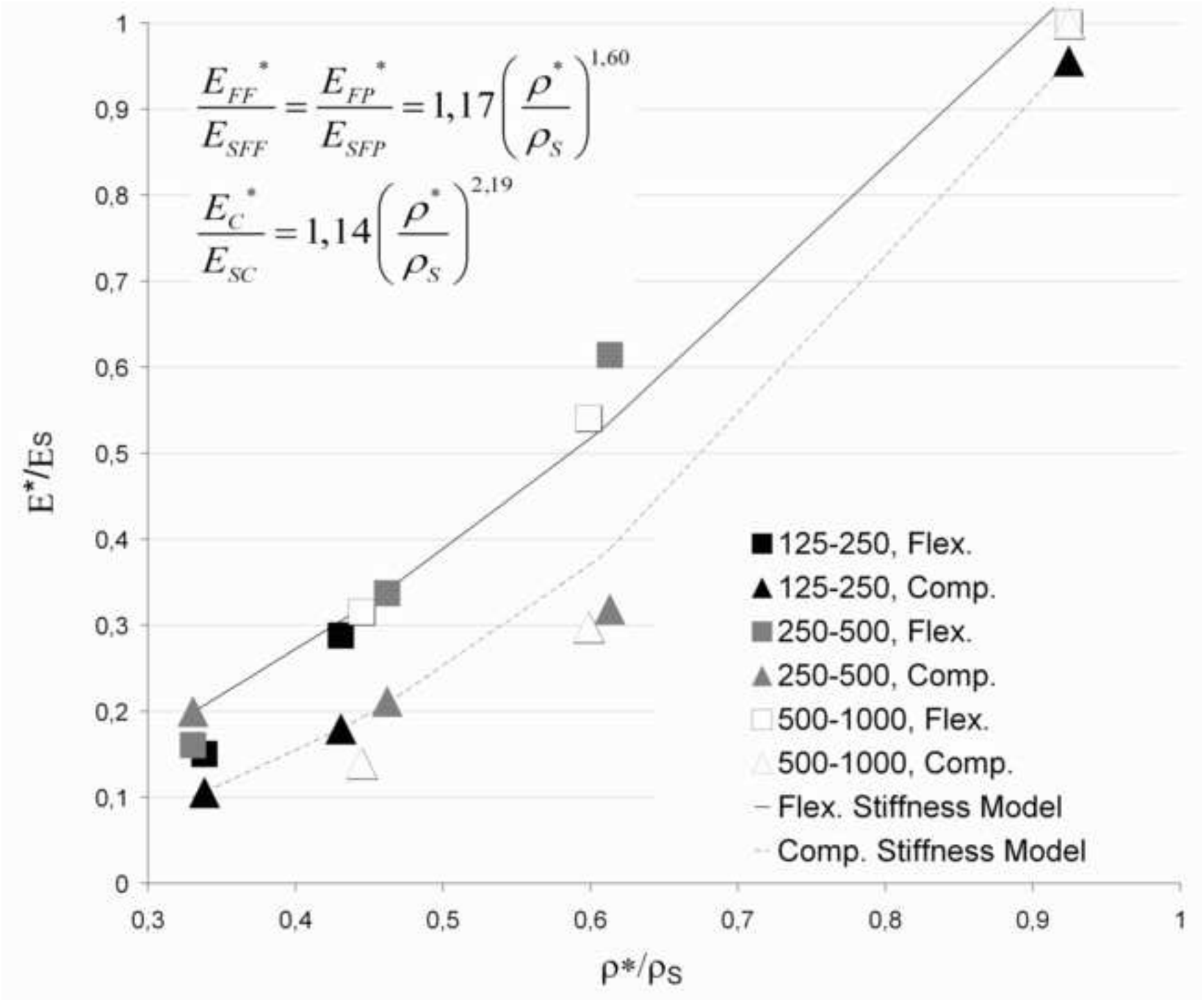
Click here to download high resolution image